State-dependent Inactivation of K^+ Currents in Rat Type II Alveolar Epithelial Cells

THOMAS E. DECOURSEY

From the Department of Physiology, Rush Presbyterian St. Luke's Medical Center, Chicago, Illinois 60612–3864

ABSTRACT Inactivation of K^+ channels responsible for delayed rectification in rat type II alveolar epithelial cells was studied in Ringer, 160 mM K-Ringer, and 20 mM Ca-Ringer. Inactivation is slower and less complete when the extracellular K^+ concentration is increased from 4.5 to 160 mM. Inactivation is faster and more complete when the extracellular Ca^{2+} concentration is increased from 2 to 20 mM. Several observations suggest that inactivation is state-dependent. In each of these solutions depolarization to potentials near threshold results in slow and partial inactivation, whereas depolarization to potentials at which the K^+ conductance, g_K, is fully activated results in maximal inactivation, suggesting that open channels inactivate more readily than closed channels. The time constant of current inactivation during depolarizing pulses is clearly voltage-dependent only at potentials where activation is incomplete, a result consistent with coupling of inactivation to activation. Additional evidence for state-dependent inactivation includes cumulative inactivation and nonmonotonic recovery from inactivation. A model like that proposed by C.M. Armstrong (1969. *J. Gen. Physiol.* 54: 553–575) for K^+ channel block by internal quaternary ammonium ions accounts for most of these properties. The fundamental assumptions are: (*a*) inactivation is strictly coupled to activation (channels must open before inactivating, and recovery from inactivation requires passage through the open state); (*b*) the rate of inactivation is voltage-independent. Experimental data support this coupled model over models in which inactivation of closed channels is more rapid than that of open channels (e.g., Aldrich, R.W. 1981. *Biophys. J.* 36:519–532). No inactivation results from repeated depolarizing pulses that are too brief to open K^+ channels. Inactivation is proportional to the total time that channels are open during both a depolarizing pulse and the tail current upon repolarization; repolarizing to more negative potentials at which the tail current decays faster results in less inactivation. Implications of the coupled model are discussed, as well as additional states needed to explain some details of inactivation kinetics.

INTRODUCTION

The K^+ channels responsible for delayed rectification in excitable cells have long been known to inactivate slowly under maintained depolarization, and to recover

Address reprint requests to Dr. Thomas E. DeCoursey, Department of Physiology, Rush Presbyterian St. Luke's Medical Center, 1750 West Harrison Avenue, Chicago, IL 60612-3864.

J. GEN. PHYSIOL. © The Rockefeller University Press · 0022-1295/90/04 /0617/30 $2.00
Volume 95 April 1990 617–646

from inactivation upon hyperpolarization, in node of Ranvier (Frankenhaeuser and Waltman, 1959; Lüttgau, 1960), squid axons (Moore, 1959; Ehrenstein and Gilbert, 1966), eel electroplaques (Bennet and Grundfest, 1966), Purkinje fibers (Hall et al., 1963); neurons from *Onchidium* (Hagiwara et al., 1961), puffer fish (Nakajima and Kusano, 1966), *Aplysia* (Alving, 1969), *Helix* (Neher and Lux, 1971; Magura et al., 1971), *Anisodoris* and *Archidoris* (Conner and Stevens, 1971*a*); and in skeletal muscle from frog (Nakajima et al., 1962; Adrian et al., 1966, 1970*b*), snake (Heistracher and Hunt, 1969*a*), rat (Duval and Leoty, 1978), and crab (Mounier, 1979). Regardless of how many distinct subtypes of K^+ channels are represented in these preparations, inactivation appears to be a common feature of depolarization-activated K^+ channels. By analogy with the Hodgkin-Huxley (1952) model for sodium channel gating, Frankenhaeuser (1963) described K^+ channel inactivation as a first-order variable which is independent of activation, thus:

$$I_K = \bar{g}_K n^2 k(V - V_K),$$

where I_K is K^+ current, $\bar{g}_K$ is the maximum available K^+ conductance, V_K is the K^+ reversal potential, and n^2 and k are variables describing the probability that a channel is activated and not inactivated, respectively. Since then it has become apparent that the kinetics of inactivation and recovery of K^+ currents are complex in a variety of excitable cells (Nakajima and Kusano, 1966; Heistracher and Hunt, 1969*b*; Neher and Lux, 1971; Schwarz and Vogel, 1971; Argibay et al., 1973; Argibay, 1974; Kostyuk et al., 1975; Heyer and Lux, 1976; Adrian and Rakowski, 1978; Aldrich et al., 1979; Dubois, 1981; Inoue, 1981; Ruben and Thompson, 1984; Chabala, 1984; Plant, 1986; Maruyama, 1987; Clark et al., 1988; Giles and Imaizumi, 1988; Kostyuk and Martynyuk, 1988; Clay, 1989) and more recently, also in nonexcitable cells (Cahalan et al., 1985; Gallin and Sheehy, 1985; Maruyama, 1987; Grissmer and Cahalan, 1989; Lucero and Pappone, 1989), suggesting additional states. In some preparations multiple kinetic components may reflect the presence of more than one K^+ channel type in the same cell (e.g., Stanfield, 1970; Duval and Leoty, 1978; Dubois, 1981; Quandt, 1988; Hoshi and Aldrich, 1988).

Several phenomena have been described which indicate that inactivation is not independent of activation, i.e., that the rates of inactivation of open and closed channels are different (Neher and Lux, 1971; Argibay et al., 1973; Argibay and Hutter, 1973; Argibay, 1974; Heyer and Lux, 1976; Eckert and Lux, 1977; Aldrich et al., 1979; Beam and Donaldson, 1983; DeCoursey et al., 1984; Clark et al., 1988). Among these, cumulative inactivation and nonmonotonic recovery from inactivation (which are described more completely in Results) can be modeled by assuming that closed channels inactivate faster than open channels (Aldrich, 1981). Inactivation of K^+ currents in rat type II alveolar epithelial cells is described here. Although two types of K^+ channels have been described, in most alveolar epithelial cells the behavior of the g_K is consistent with the predominance of a single type of K^+ channel (DeCoursey et al., 1988). In alveolar epithelial cells, closed K^+ channels appear to inactivate more slowly than open channels or not at all, and open channel inactivation appears to be relatively independent of voltage. Therefore, a model is explored which incorporates two fundamental assumptions: (*a*) closed channels do not inactivate, and (*b*) the rate of inactivation of open channels is independent of voltage. This

simple model can predict the general features of K^+ channel inactivation, including cumulative inactivation and nonmonotonic recovery kinetics.

The applicability of the proposed model is extended by use of two interventions which alter inactivation kinetics of some K^+ channels: increased extracellular K^+ concentration, $[K^+]_0$, and increased extracellular Ca^{2+} concentration, $[Ca^{2+}]_0$. Inactivation kinetics are modified by extracellular permeant cations (Lüttgau, 1961; Plant, 1986; Grissmer and Cahalan, 1989), and inactivation is diminished (i.e., inactivation is slower and/or recovery is enhanced) by elevated $[K^+]_0$ in some preparations (Ruben and Thompson, 1984; Kostyuk and Martynyuk, 1988; Martynyuk and Teslenko, 1988; Grissmer and Cahalan, 1989) excluding squid (Inoue, 1981; Clay, 1989). Increased $[Ca^{2+}]_0$ speeds inactivation of K^+ currents in node of Ranvier (Lüttgau, 1960) and in lymphocytes (DeCoursey et al., 1985; Grissmer and Cahalan, 1989) but not in squid (Inoue, 1981), in addition to shifting activation to more positive potentials (Frankenhaeuser and Hodgkin, 1957). These two actions of Ca^{2+} appear to be independent, since different polyvalent cations, all of which shift activation to more positive potentials, have qualitatively different effects on the inactivation rate, some increasing and some decreasing the inactivation time constant (DeCoursey et al., 1985). The effects of elevated $[K^+]_0$ and $[Ca^{2+}]_0$ on inactivation of type II cell K^+ currents are shown to be generally compatible with the coupled model.

METHODS

Type II Cell Isolation

Methods for isolation and purification of type II cells are adapted from those of Simon et al. (1986) as described previously (DeCoursey et al., 1988), with several modifications. The lavage solution, which was used to remove nonadherent macrophages, contained divalent-free Hank's balanced salt solution (Gibco Laboratories, Grand Island, NY) and 2% penicillin-streptomycin solution (Gibco Laboratories). The digestive enzyme solution, used to dissociate individual alveolar epithelial cells, contained 12.6 U/ml porcine pancreatic elastase (Sigma Chemical Co., St. Louis, MO), 25 μg/ml trypsin, (Sigma Chemical Co.), 20 mM HEPES, Dulbecco's modified Eagle's media (D-MEM, Gibco Laboratories). The solution instilled to arrest enzymatic activity contained 0.5 mg/ml soybean trypsin inhibitor (Sigma Chemical Co.), 60 μg/ml DNAase (Sigma Chemical Co.), fetal bovine serum (Gibco Laboratories), 2% penicillin-streptomycin solution (Gibco Laboratories), and D-MEM. The lectin solution which subsequently agglutinated residual macrophages (Simon et al., 1986) contained 50 μg/ml *Griffonia simplicifolia* lectin (Sigma Chemical Co.), 10% fetal bovine serum, and 2% penicillin-streptomycin solution. Cells were studied up to ~4 wk after isolation.

Recording Techniques

Conventional gigohm seal recording techniques as reported previously (DeCoursey et al., 1988) were used. Pipettes were made from 0010, KG-12, or EG-6 glass (Garner Glass Co., Claremont, CA), coated with Sylgard 184 (Dow Corning Corp., Midland, MI), and fire-polished to tip resistances measured in Ringer's solution of 1.5–4 MΩ. Pipette (internal) and bath (external) solutions are listed in Table I. Data were corrected for junction potentials, V_{jct}, as described in Table I, calculated assuming mobilities and activity coefficients from Robinson and Stokes (1965), Vaný́sek (1987), or Landolt-Börnstein (1960). Since all pipette solutions

contain 11 mM EGTA, it is unlikely that inactivation was contaminated by voltage-dependent block by heavy metal ions leached from the pipette glass (Cota and Armstong, 1988). Experiments were generally done at 19–22°C, with bath temperature controlled using Peltier devices and continuously monitored by a small thin-film platinum resistance temperature detector (RTD) element (Omega Engineering, Stamford, CT).

After the whole-cell configuration was established, the relative amplitudes of the leak and K^+ conductances were determined. Cells with large leak currents were not further studied. The maximum K^+ conductance seemed to be larger in this study than the average value of 1.6 nS reported previously (DeCoursey et al., 1988). This increase may reflect improvements in the cell isolation and purification techniques, or use of larger cells and cells cultured for longer times. Since we previously found two distinct types of voltage-gated K^+ channels in rat type II cells, the predominant type of K^+ channel in each cell was determined. The vast majority of cells had type *n* or delayed rectifier-type K^+ channels. As was found previously,

TABLE I

Composition of Solutions

	Intracellular (pipette) solutions								
	K^+	Ca^{2+}	Mg^{2+}	Cl^-	F^-	$CH_3SO_3^-$	EGTA	HEPES	V_{jct}
					mM				*mV*
KF	162	1	2	6	140	0	11	10	9.0
KF + KCl	162	1	2	76	70	0	11	10	6.7
KCH_3SO_3 + KF	162	1	2	6	40	100	11	10	4.6
KCH_3SO_3	162	1	2	6	0	140	11	10	10.5

	Extracellular (bath) solutions						
	Na^+	K^+	Ca^{2+}	Mg^{2+}	Cl^-	HEPES	V_{jct}
			mM				*mV*
Ringer	160	4.5	2	1	170.5	5	0
K-Ringer	0	160	2	1	170.5	10	4.6
20 Ca-Ringer	140	4.5	20	1	186.5	5	−2.2

V_{jct} is the junction potential calculated for the pipette solution/Ringer interface or the interface between the bath electrode with its Ringer-agar bridge and the bath solution when changed from Ringer. The value for the pipette solution less that for the bath solution was subtracted from the nominal potential; e.g., for KF + KCl and K-Ringer, the correction would be 6.7 − 4.6 = 2.1 mV. The pH of all solutions was adjusted with the hydroxide of the predominant cation to 7.2 for internal solutions and 7.4 for external solutions.

only a small fraction had type *l* K^+ channels, although the frequency of cells with type *l* channels seemed lower in the present experiments. Classification of a cell as having type *n* channels was based on (*a*) accumulation of inactivation during repetitive brief depolarizations, (*b*) slow tail current kinetics, and (*c*) activation at relatively negative potentials, compared with type *l;* tentative classification of a cell as having type *l* channels was confirmed by testing its sensitivity to externally applied tetraethylammonium which blocks type *l* K^+ channels at submillimolar concentrations (DeCoursey et al., 1987, 1988). All data described here are derived from type II cells judged to have type *n* K^+ channels.

K^+ currents were corrected for leak current estimated by linear extrapolation of the time-independent current at subthreshold potentials. In many cells an additional slowly activating conductance which reversed near 0 mV was observed at positive potentials, typically above +20 to +40 mV. When present, this conductance contaminated the time course of inactivation, and restricted the voltage range over which reliable data could be obtained. The series

resistance compensation was adjusted (typically ~50% compensation could be used) at the start of each experiment and periodically thereafter. In a cell with unusually large currents, such as the one in Fig. 1, the largest error due to residual uncompensated series resistance would be <10 mV, assuming a high-resistance pipette and a doubling of pipette resistance after achieving whole-cell configuration.

RESULTS

The results will be presented in four main parts. First, effects of elevated $[K^+]_0$ and $[Ca^{2+}]_0$ on K^+ channel inactivation in type II alveolar epithelial cells are described.

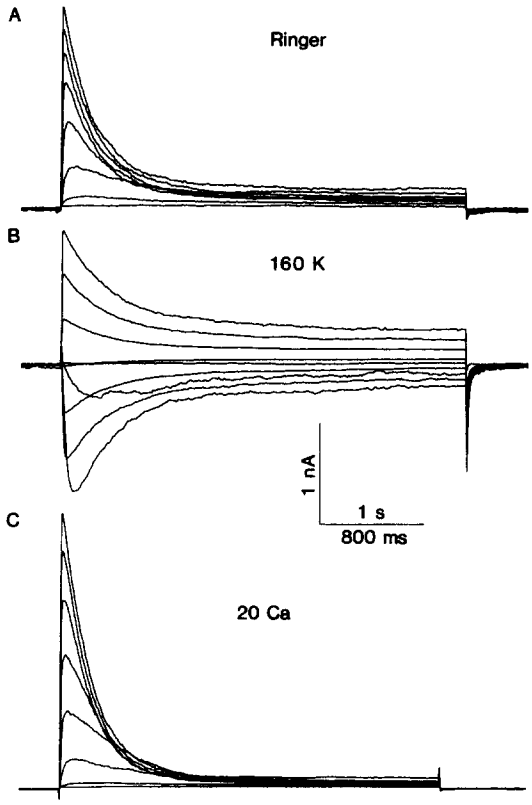

FIGURE 1. Whole-cell currents in a type II cell with unusually large currents bathed in Ringer (*A*), K-Ringer (*B*), or 20 Ca-Ringer (*C*). In *A*, the cell was held at −90 mV and 4-s pulses to −50 through +20 mV were given in increments of 10 mV with an interval of 40 s between pulses. In *B* the cell was held at −85 mV and pulsed to −45 through +35 mV in 10-mV increments, with a 30-s interval between pulses. In *C* the cell was held at −92 mV and 3-s pulses were applied to −42 through +28 mV in 10-mV increments with a 40-s interval. The calibration bars in *B* also apply to *A* and *C*, with the time calibration 800 ms for *C* only. The family in *A* was recorded after 2.5 h in whole-cell configuration, *B* after 1.5 h, and *C* after 2 h. Currents are shown without leak correction. Pipette solution KCH_3SO_3 + KF, 21°C, cell no. 531.

Then a model of channel gating and its application to the data are introduced. Various features of the data which suggest coupling of activation and inactivation are discussed. Finally, several experiments designed to discriminate between two classes of coupled models are described.

Effects of $[K^+]_0$ and $[Ca^{2+}]_0$ on K^+ Current Inactivation

Fig. 1 illustrates some of the effects of $[K^+]_0$ and $[Ca^{2+}]_0$ on K^+ channel inactivation in a rat type II cell: during long depolarizing pulses in Ringer (*A*), 160 mM K-Ringer (K-Ringer) (*B*), or 20 mM Ca-Ringer (20 Ca-Ringer) (*C*), the K^+ current rises

rapidly and then declines slowly, with an approximately exponential time course. In some experiments, a single exponential does not provide a very good fit to the decay of K^+ currents, but the deviation from a single exponential was not resolved into a consistent pattern. Time constants from the experiment in Fig. 1 are plotted in Fig. 2 *A* for all three external solutions. In each solution the rate of inactivation is slow at potentials just above the threshold for activating the K^+ conductance, g_K, and faster at more positive potentials. The time constant of inactivation, τ, is at most only weakly voltage-dependent at potentials at which the g_K is more completely activated. Inactivation is slower in K-Ringer than in Ringer; τ in the positive potential range averaged 320 ms in Ringer and 500 ms in K-Ringer in this cell. Increasing $[Ca^{2+}]_0$

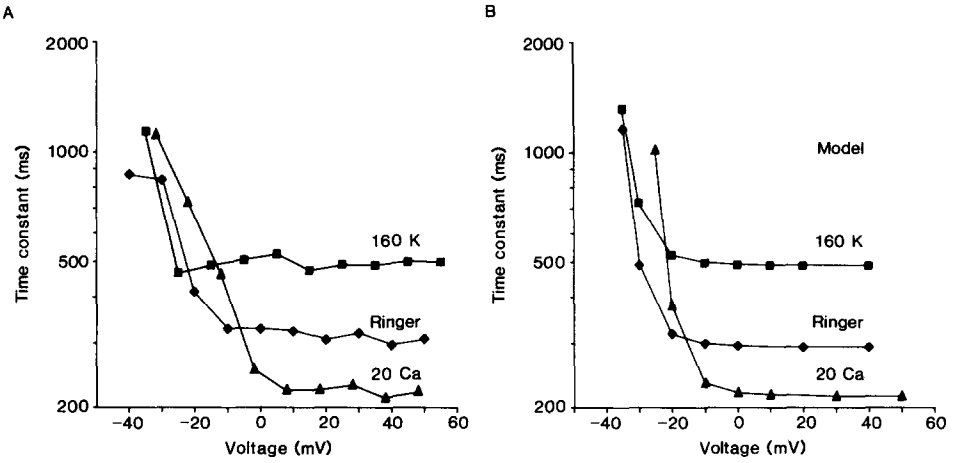

FIGURE 2. (*A*) Inactivation time constants obtained by fitting the currents in Fig. 1 to a single exponential (■, K-Ringer; ♦, Ringer; ▲, 20 Ca-Ringer). (*B*) Time constants of inactivation calculated with the model assuming voltage-independent rate constants for the $O \leftrightarrow I$ transition. The inactivation rate constants (h and j) used in the calculation were derived from the experiment in Fig. 1: for K-Ringer $h = 1.6\ s^{-1}$ and $j = 0.4\ s^{-1}$, for Ringer $h = 3.13\ s^{-1}$ and $j = 0.2\ s^{-1}$, and for 20 Ca-Ringer $h = 4.45\ s^{-1}$ and $j = 0.0909\ s^{-1}$. The surface charge effects of 20 Ca-Ringer were modeled by shifting the voltage dependence of K^+ channel activation kinetics by 10 mV to more positive potentials. The time constants were obtained by running the model, and then fitting the time course of decay of the open-state probability with a single exponential.

from 2 to 20 mM (Fig. 1 *C* and Fig. 2 *A*, ▲) speeds inactivation, with τ limiting at positive potentials to 220 ms.

Another effect of elevated $[K^+]_0$ illustrated in Fig. 1 is that inactivation in K-Ringer is less complete than in Ringer. Inactivation in Ringer was substantially complete at potentials where g_K was fully activated; the K^+ currents decayed to ~6% of their peak value. Inactivation in K-Ringer proceeded to a steady-state level of ~20% of the peak amplitude of the current. In most experiments, the rate and completeness of inactivation increased with time after establishing the whole-cell configuration, as has been described for lymphocyte K^+ currents (Fukushima et al., 1984; Cahalan et al., 1985; Deutsch et al., 1986). However, inactivation remained incom-

plete in K-Ringer, even in experiments lasting several hours. Measurements of the tail currents after repolarization in Fig. 1 *B* confirm that the currents at the end of the 4-s pulses in K-Ringer reflect K^+ current. After long pulses to potentials at which g_K is fully activated, the tail amplitude at −80 mV was ~1.0–1.2 nA. The tail current elicited by a brief depolarizing pulse in this cell had an amplitude of 6.0 nA, so ~20% of the g_K remained activated (and not inactivated) after the pulses in Fig. 1 *B*. Inactivation in K-Ringer was incomplete even in cells held at 0 mV, since tail currents could be elicited by hyperpolarizing pulses. That inactivation is incomplete even in Ringer is apparent when Ringer is replaced with 20 Ca-Ringer, which reduces the residual noninactivating current levels close to leak current. Residential noninactivating current both in Ringer and in 20 Ca-Ringer can be blocked by several K^+ channel blockers (Jacobs, E. R., and T. E. DeCoursey, manuscript in preparation).

TABLE II

Inactivation and Recovery Rate Constants at 20°C

Bath	τ	$R(I_{ss}/I_{peak})$	h	j
	ms			s^{-1}
Ringer (21)	369 ± 204	0.051 ± 0.031	3.4 ± 2.0	0.16 ± 0.11
K-Ringer (10)	736* ± 567	0.22‡ ± 0.13	1.5‡ ± 1.1	0.36‡ ± 0.26
20 Ca-Ringer (9)	198* ± 57	0.021‡ ± 0.013	5.3* ± 1.5	0.11 ± 0.07

Means ± SD are given for the number of cells in parentheses. For each cell, τ was measured at several potentials by fitting the current decay with a single exponential. The parameter R is the ratio of steady-state K^+ current (measured at the end of long depolarizing pulses) to the peak current at that potential. Pulse duration was fixed according to the inactivation kinetics in a given experiment, and was typically 1.6–4 s in Ringer, 4–10 s in K-Ringer, and 1–2 s in 20 Ca-Ringer. Values of h and j were calculated for each current record from τ and R as described in the text. The values for each of the four parameters in the table were averaged for each cell, because all four parameters appear to be voltage-independent at potentials at which the g_K was fully activated, usually ~0 mV to +50 mV. The average ratio of τ(0 mV)/τ(+40 mV) is 1.12 in Ringer, 1.07 in K-Ringer, and 1.11 in 20 Ca-Ringer. Values for τ, h, and j from a few cells studied at >1°C away from 20°C were corrected to 20°C assuming a Q_{10} of 4.0 obtained in preliminary measurements around 20°C. The Ringer data were collected on average 35 min after whole-cell configuration was established, the K-Ringer data at 76 min, and the 20 Ca-Ringer data at 75 min. *$P < 0.05$ vs. Ringer. ‡$P < 0.01$ vs. Ringer.

The effects of $[K^+]_0$ and $[Ca^{2+}]_0$ on inactivation kinetics are summarized in Table II. The time constant, τ, of the decay of current during depolarizing pulses which fully activate g_K is highly variable from cell to cell, averaging 369 ms in Ringer with a range of 104–757 ms. Some of this variability results from the progressive decrease in τ with time in the whole-cell configuration, which can be a twofold change over the course of a long experiment. However, in some cells inactivation was unusually slow throughout the experiment and in others it was fast at all times, so there seems to be a substantial contribution of cell-to-cell variability. In K-Ringer τ is also quite variable, with a range of 227–2,210 ms. When studied in a given cell, however, τ is consistently larger in K-Ringer than in Ringer, by an average of about twofold. 20 Ca-Ringer consistently reduces τ to an average of about half of its value in Ringer.

The completeness of inactivation was quantified by taking the ratio, R, of the steady-state current, I_{ss}, to the peak current, I_{peak}, during long depolarizing pulses (up to 8 s). Mean values of parameter R in a number of cells are plotted in Fig. 3 *A*. In all three solutions, R is large in the voltage region in which the g_K is only partially activated, and decreases to a practically constant value at potentials where the g_K is fully activated. It appears that R is independent of potential at positive potentials where the g_K is fully activated. However, it cannot be ruled out that R may depend weakly on potential. In many cells the appearance of a slowly activating conductance at large positive potentials limited the voltage range over which this parameter could be estimated, and R was especially subject to errors in Ringer and 20 Ca-Ringer where it is numerically small and dependent on accurate leak subtraction. Inactivation is less complete in K-Ringer compared with Ringer, the mean noninactivated

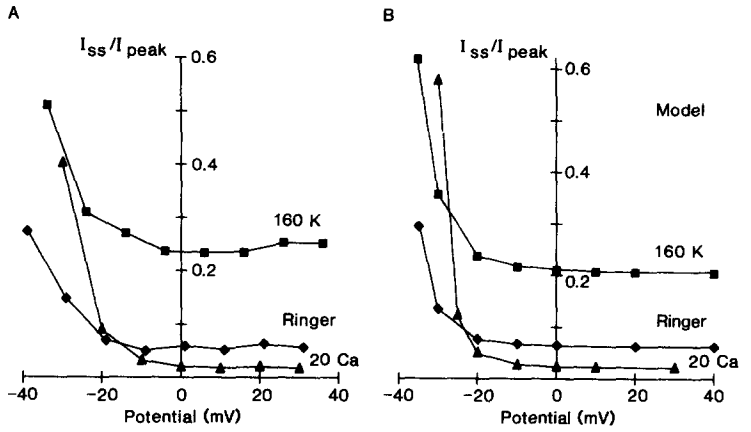

FIGURE 3. (*A*) Mean values of R, the steady-state noninactivating K^+ current (I_{ss}) as a fraction of peak current (I_{peak}) at each potential, in K-Ringer (■, n = 6–9), Ringer (♦, n = 7–10), and 20 Ca-Ringer (▲, n = 4–8). Steady-state current was measured at the end of pulses ranging from 1 to 8 s depending on the inactivation τ in each cell and each solution. (*B*) Calculated values for the noninactivating component, R, from the simulations described in Fig. 2 *B*. This parameter was derived from model currents in the same way as it was derived from real data, as the ratio of the steady-state current at each potential to the peak current, during the calculated response to depolarizing voltage steps.

component increasing from 5% to 22% (Table II). Increasing $[Ca^{2+}]_0$ to 20 mM decreases R to barely measurable levels, averaging 0.02. Measured values of τ and R were used to derive apparent rate constants of inactivation, h, and recovery, j, as will be described in the next section.

The pronounced lessening of K^+ channel inactivation in elevated $[K^+]_0$ is obvious when brief depolarizing pulses are applied repetitively. Currents in Ringer during successive 100-ms pulses to +20 mV repeated at 1 Hz decrease progressively by >50% as inactivation accumulates. In K-Ringer a similar pulse train results in only slight inactivation, averaging <20%, and in some cells negligible inactivation accumulates. In 20 Ca-Ringer accumulation of inactivation is more pronounced than in Ringer, with an average decrease of 85%.

The Model

In the section immediately following this one, experimental evidence will be presented which suggests that (*a*) activation and inactivation are not independent, (*b*) inactivaton of closed channels is sufficiently slow to be neglected, and (*c*) the rate at which open channels inactivate is relatively independent of membrane potential. The simplest possible coupled model which incorporates these observations is therefore considered in order to explore the implications of such a model and to determine the extent to which this model can describe the data:

$$C_{1-4} \rightleftharpoons O \underset{j}{\overset{h}{\rightleftharpoons}} I.$$

In this model inactivation is "coupled" to activation, i.e., the inactivated state, I, (or states, see Discussion) can be accessed only from the open state, O, and recovery from inactivation must occur via the open state. This model is analogous to Armstrong's (1969) model for block of K^+ channels by internal quaternary ammonium ions.

The probability of occupancy of the various states was calculated numerically as a function of time, based on initial conditions and the rates of entry or exit from each state. The total probability of occupancy of all states was set at unity; for example, an occupancy value of 0.3 means that 30% of all channels are in that state. The time increment of the calculation was usually 0.1–1 ms, depending on the rate constants at the voltages in the calculation. Calculations were usually started from a "holding potential" of −80 mV at which all channels are in the deepest closed state, C_1 (see below). For voltage pulses in the calculation all rate constants were determined from empirically estimated continuous functions of membrane potential, which are described below. Currents were calculated simply as the product of the open probability and $(V - V_K)$, without any assumed open-channel current rectification.

*Activation.*The voltage dependence of K^+ channel opening and closing kinetics for the calculations are based on the Hodgkin-Huxley (1952) n^4 model, with its four independent gating "particles." Several more complex models have been proposed which provide a more accurate description of K^+ channel gating behavior (Cole and Moore, 1960; Gilly and Armstrong, 1982; White and Bezanilla, 1985), but for the present purposes an approximate predictor of the time-course of open and closed channel states is all that is required. In addition, the Hodgkin-Huxley model facilitates extraction of rate constants from experimental data and expression of these rate constants as continuous functions of voltage. The voltage-dependence of the forward and backward rate constants, α and β respectively, were built into the model and not further adjusted for each simulation, except where noted. K^+ channel activation kinetics are described by:

$$C_1 \underset{\beta}{\overset{4\alpha}{\rightleftharpoons}} C_2 \underset{2\beta}{\overset{3\alpha}{\rightleftharpoons}} C_3 \underset{3\beta}{\overset{2\alpha}{\rightleftharpoons}} C_4 \underset{4\beta}{\overset{\alpha}{\rightleftharpoons}} O,$$

where $C_1 \ldots C_4$ are four nonconducting (closed) states, O is the conducting (open) state. The voltage-dependence of α and β for all calculations except those simulating

20 Ca-Ringer, is given by:

$$\alpha = 8.6 \frac{V + 25}{1 - \exp\left[\frac{-25 - V}{3.6}\right]} \quad (1)$$

$$\beta = 1.5 \exp\left[\frac{-25 - V}{26}\right] \quad (2)$$

where V is the potential in millivolts and the rate constants are in units of s^{-1}. To simulate the surface potential screening effect of 20 Ca-Ringer, the voltage dependencies of α and β were simply shifted by 10 mV to more positive potentials. The values for the parameters in these equations were adjusted so that the calculated voltage dependence of $(\alpha + \beta)^{-1}$ approximated the time constant τ_n measured in several type II cells over a wide voltage range at 20–21°C. For this purpose, values of τ_n were obtained by fitting K^+ currents during depolarizing voltage pulses to: $I_K(t) = A\ [1 - \exp(-t/\tau_n)]^4$, and by fitting tail currents following a large depolarizing prepulse to: $I_K(t) = A \exp(-4t/\tau_n)$, with adjustable parameters amplitude (A) and τ_n. It is assumed that g_K is negligibly small at the holding potential of ~ -90 mV from which the depolarizing pulses were given, and that g_K was saturated during the large depolarizing pulse which preceded the tail currents. It seemed preferable to establish one (albeit arbitrary) set of gating parameters (i.e., Eqs. 1 and 2) to be used in all calculations, rather than to adjust all the parameters for each cell; this decision results in slight differences in the voltage dependence of calculated channel gating when compared with data from any given experiment. Since transitions between inactivated and closed channels are not allowed in the model, transitions between closed states and even the number of closed states are not critical to the calculations, and the occupancy of the four nonconducting closed states is lumped: $C = C_{1-4} = C_1 + C_2 + C_3 + C_4$. The model generates reasonable voltage and time dependencies of occupancy of open, O, and combined closed, C_{1-4}, states.

Inactivation. At potentials at which the g_K is maximally activated, the $O \leftrightarrow I$ relaxation can be considered in isolation, because the $C \leftrightarrow O$ equilibrium is maximally displaced towards state O. In this potential range the observed time constant of current decay, τ, reduces to $1/(h + j)$, and the noninactivating component, R, is approximately $j/(h + j)$. The rate constants h and j can therefore be calculated for each current record: $h \approx (1 - R)/\tau$ and $j \approx R/\tau$. Values for h and j estimated in this way for currents at various potentials in a number of cells are summarized in Table II. When the voltage range is restricted to that at which the g_K is fully activated, τ and R, and therefore also h and j, are independent of voltage, within the resolution of the data, in all three external solutions. Since R is small and hard to determine in Ringer and especially 20 Ca-Ringer, the values obtained for j are only approximate. The validity of the extraction of h and j was tested since several simplifying assumptions are involved. Model currents were generated using parameter values typical of Ringer, K-Ringer, and 20 Ca-Ringer; τ and R were measured; and h and j were extracted as they were from real data. The resulting values of the two rate constants were in reasonable agreement with the original ones.

The results summarized in Table II indicate that increasing $[K^+]_o$ to 160 mM decreases the inactivation rate h and increases the recovery rate j, both factors leading to a larger residual noninactivating component, R. Elevated $[Ca^{2+}]_o$ increases h, but without significantly reducing j compared with values in Ringer, resulting in a smaller residual component. The rate constants in Table II are clearly model-dependent. Preliminary data, as well as data in the literature (references given in the Introduction), suggest that recovery from inactivation often occurs with at least two components, so that modeling recovery using a single rate constant is an oversimplification. More complete models with two inactivated states are considered in the Discussion.

Evidence That Inactivation Is Coupled to Activation

The inactivation rate is voltage-independent. In a sequential (i.e., coupled) reaction scheme in which the first step equilibrates much faster than the second, the slower observed time constant will be slowed when the first step considered in isolation does not proceed to completion (Bernasconi, 1976). Thus, in a coupled model even if the rate of inactivation were completely voltage-independent, the observed time constant of inactivation would vary, decreasing at more positive potentials in the voltage range in which g_K is only partly activated. Fig. 2 *A* shows that in type II cells this pattern is observed for inactivation in Ringer, 20 Ca-Ringer, and K-Ringer. Fig. 2 *B* illustrates the voltage dependence of τ in the coupled model, with voltage-independent rate constants of inactivation, h and j. The voltage dependence of τ predicted by the model is quite similar to that observed in all three solutions.

Inactivation is slow at potentials where K^+ channels are closed. The rate of inactivation of open channels could be estimated directly from the decay of current at positive potentials where the g_K was fully activated. The rate of inactivation at potentials near the threshold for activation of g_K was studied by applying a prepulse of varying duration followed by a constant depolarizing test pulse. Fig. 4 illustrates this type of experiment both in Ringer (*A*) and in K-Ringer (*B*). In the lower panel of Fig. 4 *A* the test pulse after an 8-s prepulse to −40 mV elicits a current indistinguishable from that without a prepulse. Inactivation at −40 mV is thus either very slow or negligible. A prepulse to −30 mV (*second panel*) causes a slow and partial inactivation of the g_K, as evidenced by the decreased amplitude of the current during the test pulse to 0 mV. The inactivation caused by prepulses to −20 mV is faster and more complete (*top panel*). The prepulses to −30 and −20 mV elicit slowly inactivating outward currents which can be fit approximately with single exponentials of 760 and 670 ms, respectively. When τ is estimated from the envelope of test currents fit to a single exponential, τ is somewhat larger, being 1.8 and 1.0 s for −30 and −20 mV, respectively. At −20 mV the envelope is better fitted by the sum of two exponentials, with time constants 400 ms and 2.4 s. These results suggest at least one additional inactivated or open state must exist, consistent with results in a variety of cell types mentioned in the Introduction.

Fig. 4 *B* illustrates analogous measurements in the same cell in K-Ringer, with similar results. An 8-s prepulse to −45 mV elicits neither detectable K^+ current during the prepulse nor inactivation judged by the test pulses to +25 mV. More positive prepulses elicit inactivating inward K^+ current during the prepulse, and the

test pulse envelopes reveal slow and partial inactivation at −35 mV and faster and more complete inactivation at −25 mV. Estimated from the decay of prepulse currents, τ is 1.0 s and 340 ms at −35 and −25 mV, respectively, estimates of τ from the test pulse envelope being 1.2 s and 580 ms. The envelope for the −25-mV envelope is better fitted by two components, with time constants 230 ms and 2.8 s. This type of experiment indicates that inactivation of closed channels at subthreshold

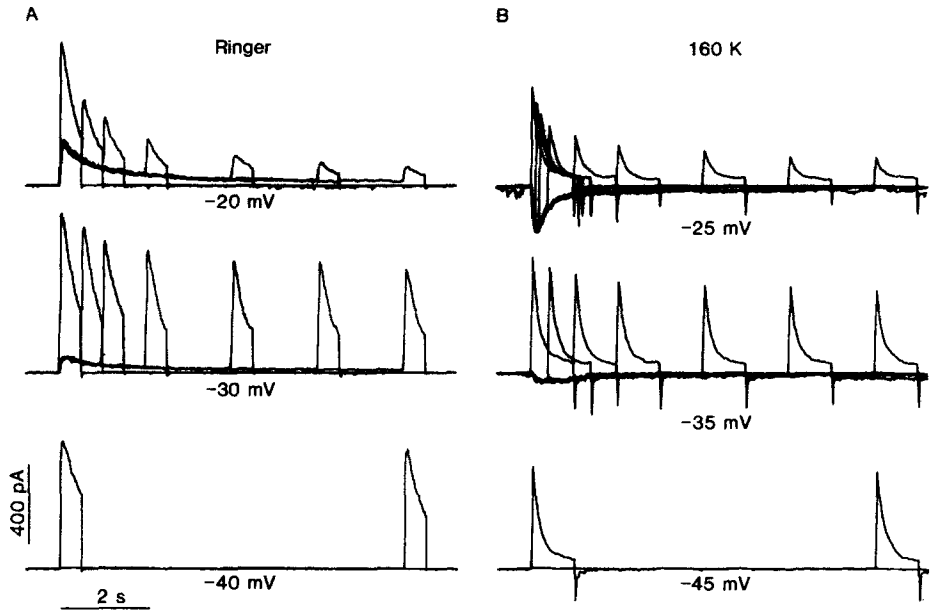

FIGURE 4. Slow onset of inactivation near the threshold for g_K activation in Ringer (*A*) and in K-Ringer (*B*). In *A*, the cell was held for >1 min at −100 mV, then a prepulse was applied to the indicated potential, immediately followed by a test pulse 500 ms long to 0 mV, to determine the extent of inactivation during the prepulse. Detectable inactivation occurs only at prepulse potentials at which the g_K is activated, as can be seen from the outward currents at −30 mV and at −20 mV during the prepulses. In each figure a test pulse without a prepulse is shown (i.e., with a 0-s prepulse duration) to show the control test current amplitude. Calibrations apply to both *A* and *B*. (*B*) An analogous experiment in the same cell in K-Ringer. Here the cell was held at −95 mV and the test pulses are 1 s long to +25 mV. Note the inward current during the prepulses to −35 and −25 mV. The measurements in *A* were made 30–60 min after whole-cell configuration was established, those in *B* were made after 120–140 min. The faster inactivation in K-Ringer compared with Ringer reflects in part the more positive test potential, and in part the progressive increase in the rate of inactivation seen in most cells (see text); τ measured in Ringer after 90 min was half of its value when the measurements in *A* were made. Pipette solution KCH_3SO_3 + KF, 21.8°C, cell no. 536.

potentials is quite slow or negligible compared with the rate of inactivation of open channels at more positive potentials. Similar experiments on skeletal muscle led Argibay et al. (1973) to the same conclusion.

Substantial inactivation occurs only at potentials where channels open. Experiments such as the one in Fig. 4 indicate that closed channels inactivate slowly, if at all, at

subthreshold potentials. Extremely slow inactivation might not have been resolved, however. Therefore, the voltage dependence of steady-state inactivation was estimated by holding the membrane at various potentials for at least 1 min and then giving a brief test pulse to a fixed potential. Fig. 5 illustrates the results of this type of measurement in Ringer (*A*), K-Ringer (*B*), and 20 Ca-Ringer (*C*). The test pulse current amplitude after 1-min prepulses is shown for each solution (■), all normalized to the test current elicited directly from the holding potential −90 mV. For comparison the normalized peak K^+ conductance during depolarizing steps without prepulses is shown (♦). In all three solutions, the holding potential had no effect on the test current (■) at potentials >~5–10 mV negative to the threshold for activating detectable K^+ currents. It was necessary to hold the cell for at least 1–2 min at ~−90 mV to allow for recovery from a holding potential which caused inactivation before proceeding with another holding potential, because recovery from inactivation was extremely slow at just subthreshold potentials (−60 to −40 mV, data not shown), as has been described elsewhere (Heistracher and Hunt, 1969*b*; Argibay, 1974; Ruben and Thompson, 1984; Cahalan et al., 1985). In other experiments partial inactivation was detected with long prepulses (5–12 min) to subthreshold potentials at which K^+ current could not be detected. Since significant inactivation could be demonstrated only within ~10–15 mV of potentials at which the g_K was clearly activated, it is not clear whether closed channels can inactivate slowly, or whether some channels open and inactivate without giving rise to detectable macroscopic currents.

There appears to be a smaller noninactivating component in the data in Fig. 5 where 1-min prepulses were used than was observed with shorter pulses (e.g., Fig. 1). In K-Ringer the noninactivating component after 1-min prepulses was 0.07 of the total, compared with 0.17 estimated in the same cell with 8-s pulses. These results may reflect the presence of an additional, slower inactivation process, but this point was not pursued.

The curves through the squares in Fig. 5 show the best-fitting Boltzmann (see legend) for the steady-state inactivation data. The voltage dependence of steady-state inactivation, measured in this way, is quite steep, with slope factors, k_j, of 2.2–6.0 mV in the three solutions. Average values for slope factors in experiments done as described in Fig. 5 are Ringer 3.5 ± 0.4 mV (mean ± SE, $n = 6$), K-Ringer 4.6 ± 0.5 mV ($n = 4$), and 20 Ca-Ringer 4.3 ± 0.6 mV ($n = 3$). The mean midpoint, V_j, in these experiments was −35 ± 3 mV (mean ± SD) for Ringer, −31 ± 3 mV for K-Ringer, and −31 ± 4 mV 20 Ca-Ringer. If inactivation is essentially voltage-independent and strictly coupled to activation, then the steepness of its voltage dependence should be related to that of activation. We previously reported an average slope factor for activation of the g_K in rat type II cells, fitted with a simple Boltzmann, of 5.5 mV (DeCoursey et al., 1988). As measured in Fig. 5, inactivation has a steeper voltage-dependence than does activation. Peak open probability (♦) and the probability that a channel is not inactivated (■) are plotted in Fig. 5 *D* for model "data" using typical Ringer parameters (Fig. 2 *B, legend*). The voltage dependence of activation in model data derived from the peak g_K–voltage relation, as are experimental data, has a slope factor of 4.8 mV. Steady-state inactivation in the model has a steeper voltage dependence, with a slope factor of 1.9 mV. The relationship

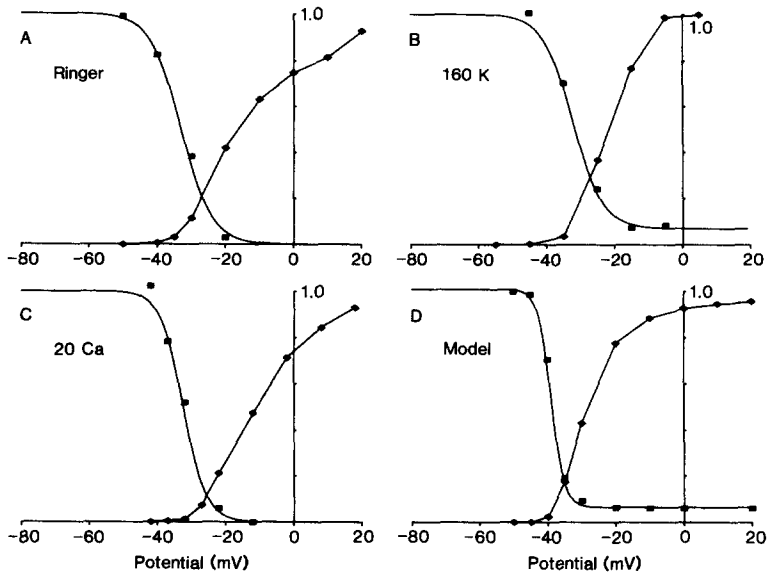

FIGURE 5. Steady-state inactivation compared with activation in a type II cell bathed in Ringer (*A*), K-Ringer (*B*), or 20 Ca-Ringer (*C*). In each part, the voltage dependence of activation (♦) was determined as the peak chord K^+ conductance normalized to the maximum value at positive potentials, without any correction for instantaneous rectification. The voltage dependence of steady-state inactivation (■) was measured by holding the cell for >1 min at ~ −90 mV, changing the holding potential to the value on the abscissae for 1 min, and then applying a single brief test pulse to ~ +10 mV. The peak current during each test pulse was normalized to that for a test pulse from a holding potential of ~ −90 mV. For the K-Ringer data, after each 1-min prepulse a brief depolarizing pulse to +35 mV was immediately followed by a test pulse to −85 mV, and the peak of the inward tail current at −85 mV was measured. The curves through the squares show the best-fit (by nonlinear least-squares) of a Boltzmann to the data:

$$I_{test}(V)/I_{test,max} = 1/\{1 + \exp[(V - V_j)/k_j]\},$$

where the maximum test current $I_{test,max}$, the potential at which half the channels are inactivated V_j, and the slope factor k_j were allowed to vary. Any noninactivating component was ignored except for the K-Ringer data, which were fitted to:

$$I_{test}(V)/I_{test,max} = (1 - I_{test,min})/\{1 + \exp[(V - V_j)/k_j]\} + I_{test,min},$$

where $I_{test,min}$ is the fitted minimum value of the test current, and was 0.07 of the value of $I_{test,max}$. Fitted parameter values in Ringer are V_j −33 mV and k_j 4.6 mV, in K-Ringer V_j −32 mV and k_j 4.4 mV, and in 20 Ca-Ringer V_j − 32 mV and k_j 3.4 mV. All data were recorded at 20.6–21.1°C, with KCH_3SO_3 + KF in the pipette, cell no. 538, with the Ringer data collected 20–40 min after establishing whole-cell configuration, the K-Ringer data at 45–65 min, and the 20 Ca-Ringer data at 100–130 min. The lack of a clear depolarizing shift in the 20 Ca-Ringer data compared with Ringer data probably indicates that a small hyperpolarizing voltage shift occurred in the time between the two sets of measurements, presumably like that reported in various other preparations (Marty and Neher, 1983; Fernandez et al., 1984; Cahalan et al., 1985); when the voltage dependence of g_K activation was compared in measurements close together in time, activation was always shifted in the positive direction by 20 Ca-Ringer. (*D*) Analogous model-generated "data" with typical Ringer parameters, τ = 300 ms and R = 0.06; ♦, peak open probability without normalization; ■, probability that channels are not inactivated in the steady state. Parameters obtained by fitting to the equation described in *B* are V_j −38.5 mV, k_j 1.91 mV, and I_{min}/I_{max} 0.064. At the end of a calculated 50-s pulse to −45 mV, the open probability is 0.00084 and still slowly rising and the probability that a channel is inactivated is 0.013, illustrating how long times at just-threshold potentials amplify the $O \rightarrow I$ transition.

between the steepness of the voltage dependence of activation and inactivation of the g_K in type II cells is thus generally compatible with a strictly coupled mechanism of the form given in the model.

Cumulative inactivation and nonmonotonic recovery from inactivation. A peculiar feature of delayed rectifier inactivation in some cells, termed "cumulative inactivation" by Aldrich et al. (1979), is that the peak current during the second of two identical depolarizing pulses can be smaller than the current at the end of the first pulse. This phenomenon has been reported for K^+ currents in snail neurons (Neher and Lux, 1971; Aldrich et al., 1979), rat skeletal muscle (Beam and Donaldson, 1983), human T lymphocytes (DeCoursey et al., 1984), "gulf" squid giant axons

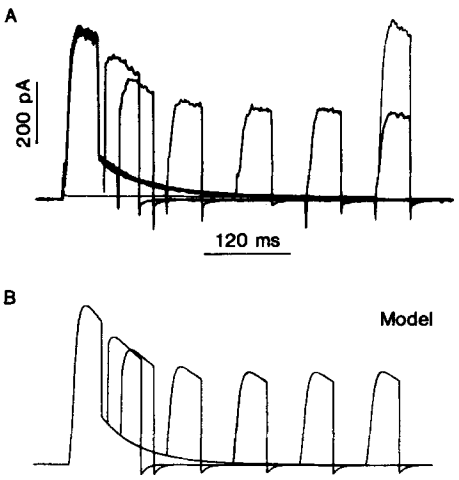

FIGURE 6. (*A*) Cumulative inactivation and apparently nonmonotonic recovery from inactivation, illustrated in a cell bathed in 20 Ca-Ringer (in which τ was faster and cumulative inactivation was more pronounced than in Ringer). Superimposed are currents recorded when from a holding potential of −92 mV the potential was stepped to +8 mV for 50 ms, then to −52 mV for various times, then again to +8 mV for 50 ms. The cell was allowed to recover at −92 mV for >60 s between measurements. In this experiment the interpulse potential of −52 mV was about 15–20 mV negative to the "threshold" at which macroscopic currents were first detectable. The lighter trace shows the current recorded when the cell was stepped directly to −52 mV, and after 450 ms to +8 mV. This shows that inactivation of closed channels at −52 mV does not account for the diminution of current during the second pulse. Note that the time course of the deepening of inactivation parallels that of the tail current. Pipette solution KCH_3SO_3 + KF, 20.4°C, cell no. 508. (*B*) Model currents for the pulse protocol in *A*. Based on τ and R measured in this experiment, 180 ms and 0.037, respectively, h was set at 5.35 s^{-1} and j at 0.206 s^{-1}. In order that the model tail current decay with about the same time course as that observed directly at −52 mV in *A*, β was set to 3 s^{-1}, otherwise standard parameters were used.

(Horrigan et al., 1987), and rabbit atrial cells (Clark et al., 1988). Fig. 6 *A* illustrates cumulative inactivation in a type II cell. Depolarizing pulse pairs were applied with various intervals between the two pulses. The cell membrane was held at −52 mV between the pulses, and was allowed to recover for at least 1 min at −92 mV before each pair was applied. The currents during the first pulse of each pair are superimposed in the figure. For each of the intervals shown, 10–400 ms, the peak current during the second pulse is smaller than the current at the end of the first pulse, i.e., there was cumulative inactivation. The lighter curve shows the test current when the potential was stepped directly to −52 mV for 450 ms and then a single test pulse

was applied. This test current is not detectably different from that without a prepulse, showing that closed channel inactivation at −52 mV is negligible for the durations of the interpulse intervals used.

Recovery from inactivation has been reported to proceed after an initial delay in some preparations (Heistracher and Hunt, 1969*b*; Adrian et al., 1970*a*; Argibay and Hutter, 1973; Argibay, 1974; Clay, 1989). If recovery is studied when only a fraction of channels are inactivated, nonmonotonic "recovery" kinetics can sometimes be observed, which gives the appearance that inactivation progresses after the end of the first pulse (Neher and Lux, 1971; Eckert and Lux, 1977; Aldrich et al., 1979). Fig. 6 *A* illustrates this phenomenon in type II cells. The decrease in the amplitude of the second pulse in each pair is greater as the interval is made longer; the time course of this deepening of inactivation mirrors that of the tail current. For much longer intervals, the current during the second pulse eventually approaches that of the first pulse, reflecting slow recovery; the currents during the first pulse essentially superimpose, indicating that recovery was practically complete during the 1-min interval between pulse pairs. In the same experiment, apparently nonmonotonic recovery was also clearly detected when the cell was held at −72 mV between pulses. The time course of the initial deepening of inactivation was faster, again mirroring that of the tail current, and the amount of deepening was less.

The experiment in Fig. 6 *A* was simulated using the coupled model, as shown in Fig. 6 *B*. Cumulative inactivation and nonmonotonic recovery kinetics are both predicted by the model, and generally resemble the phenomena observed experimentally. The time course of nonmonotonic recovery follows that of the tail current. The depth of cumulative inactivation is greater in the model, as in actual data, when the cell is held at more positive potentials between pulses. According to the present model, this occurs because channels close more slowly at positive potentials, allowing more time for open channels to inactivate during the tail current.

Cumulative inactivation is not detectable in K-Ringer, where inactivation is slow (τ is large). In Ringer, cumulative inactivation is harder to demonstrate in cells with unusually large τ, and is more profound when the membrane is repolarized to more positive potentials where τ_{tail} is slower. Finally, cumulative inactivation is enhanced in 20 Ca-Ringer, where τ is smaller than in Ringer. Although these data could be explained by other models, the simplest interpretation seems to be that (*a*) cumulative inactivation depends on the relative rates of K^+ channel inactivation and closing (i.e., approximately h compared with 4β), and that (*b*) open K^+ channels inactivate at all potentials, so that inactivation is enhanced by any intervention which increases the time channels spend in the open state.

Distinction between the Models

Aldrich (1981) showed that the phenomena of cumulative inactivation and apparently nonmonotonic recovery from inactivation can be explained by the following four-state model:

$$I_1 \rightleftharpoons C \rightleftharpoons O \rightleftharpoons I_2$$

$$Z_r \quad R \quad A \quad Z_a \text{ (Aldrich's nomenclature)}$$

in which inactivation is state-dependent, and upon depolarization closed channels

inactivate ($C \rightarrow I_1$) faster than do open channels ($O \rightarrow I_2$). In preliminary simulations this model was applied to type II cell K^+ currents by adjusting the rate constants to reflect the kinetics observed. The model provided a good description of most of the data, including cumulative inactivation and apparently nonmonotonic recovery from inactivation. However, additional data such as Figs. 2–5 suggest that alternative models must be considered in which $C \rightarrow I_1$ is slower than $O \rightarrow I_2$. The extreme form of this adjustment, in which transitions between C and I are forbidden, can account for most of the observed behavior.

In both models, the early phase of the recovery time course, during which inactivation appears to deepen (Fig. 6), follows the time course of the tail current. In the Aldrich model nonmonotonic recovery results from "protection" of the channels which are still open from undergoing the rapid $C \rightarrow I_1$ transition during a subsequent depolarization. In the present model the deepening of inactivation is due to those channels which are still open during the tail current continuing to inactivate. The continued inactivation during the tail current occurs because the inactivation rate is strictly state-dependent, but not very voltage-dependent. Although both the Aldrich model and the present coupled model can account for cumulative inactivation and nonmonotonic recovery from inactivation, the two models can be distinguished because they make different predictions which can be tested experimentally.

Do some closed channels inactivate rapidly? Cumulative inactivation can be modeled by assuming that closed channels inactivate rapidly on depolarization (Aldrich, 1981) so that a significant fraction of channels inactivate before the peak current is attained. Although Fig. 4 indicates that at subthreshold potentials closed channels inactivate quite slowly, if at all, it could be that at more positive potentials closed channels might inactivate much more rapidly. Fig. 7 illustrates an experiment to test this idea. As indicated schematically in the inset, a cell in Ringer was held at −90 mV for >60 s, then 50 brief 5-ms pulses to −10 mV were applied at ~3 Hz, immediately followed by an 80-ms pulse also to −10 mV. The current elicited by this 80-ms pulse (trace *1*) was indistinguishable from that during a single 80-ms pulse after >60-s rest at −90 mV (*lighter curve*). The 5-ms pulses in the train were short enough, as indicated by the vertical bars, that only a few channels opened. Since recovery from inactivation in Ringer is extremely slow, the lack of any accumulation of inactivation in this experiment suggests that negligible closed channel inactivation occurred at −10 mV. The currents in Fig. 7 labeled *2* and *3* were elicited by second and third 80-ms pulses to −10 mV, following the first post-train pulse after the same interval as between pulses in the train. These currents are clearly smaller than the first one, indicating that significant inactivation can accumulate for pulses to this potential, −10 mV, at this frequency. This experiment does not support the idea that significant numbers of closed channels inactivate rapidly upon depolarization. Whether closed channels might inactivate slowly during large depolarizations is hard to evaluate since most channels rapidly open, so that open channel inactivation predominates.

In order to carry out similar experiments at more positive potentials where K^+ channels open more rapidly, it was necessary to apply shorter pulses in the trains to avoid open channel inactivation. In two cells bathed in 20 Ca-Ringer, no inactiva-

tion was detected after 50 pulses to +10 mV each 1.7–2.0 ms long, but 3-ms pulses were long enough to partially activate the g_K and depress the post-train test current by 35%. A train of 50 pulses 1.4 ms long to +30 mV did not affect the test current, which was clearly reduced by a train of 2-ms pulses. These experiments provide no evidence for a rapid $C \rightarrow I$ transition.

Open K^+ channels inactivate during tail currents. Another type of experiment which helps to discriminate between the two models is illustrated in Fig. 8 *A*. Identical pulse pairs were applied in a cell bathed in 20 Ca-Ringer. During the interval between pulses, the membrane was held at either −89 or −49 mV (*dark* and *light lines*, respectively). Cumulative inactivation is observed in both cases, as the current during the second pulse does not reach the level at the end of the first pulse. However, the fraction of channels inactivated is greater when the membrane was held at −49 mV between pulses. In the Aldrich model, cumulative inactivation occurs because a significant fraction of channels are inactivated during each depolarizing

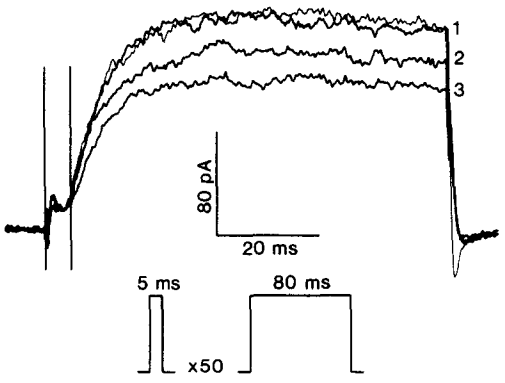

FIGURE 7. Closed channels do not inactivate rapidly during depolarization. The current shown with the lighter line was recorded during an 80-ms pulse to −10 mV after >1 min of rest at −90 mV. After >1 min at −90 mV, a train of pulses to −10 mV was applied at ~3 Hz. After 50 pulses 5 ms in duration (indicated by *vertical lines*), the pulse duration was changed to 80 ms, with the currents during the next three pulses shown. The first of the longer pulses is indistinguishable from the control recorded without a conditioning train, indicating that the 5-ms pulses did not result in detectable accumulation of inactivation. Inactivation does accumulate during the longer pulses, applied at the same frequency, ruling out the possibility that the pulse rate was too slow to allow accumulation of inactivation. Bath is Ringer, pipette KCH_3SO_3, 21.1°C, cell no. 501.

pulse via the $C \rightarrow I_1$ pathway, and recover only slowly in the interval. Since the test pulse amplitude was not changed, there should be no effect of the interpulse potential, as long as the interval is long enough to allow all open channels to close, i.e., as long as the tail current decays completely. The coupled model, on the other hand, predicts that the degree of inactivation will be greater when the cell is held at a more positive potential between test pulses, because the tail current will decay more slowly, allowing more time for open channels to inactivate. Fig. 8 *B* illustrates that the enhancement of inactivation with −49 mV interpulse potential is not due to closed channels inactivating at −49 mV. Pulses to −49 or −129 mV (*light* and *dark lines*, respectively) of the same duration as the interpulse interval in Fig. 8 *A* had no effect on the subsequent test current.

Fig. 8 *C* shows currents calculated using the coupled model for the experiment in Fig. 8 *A*. The degree of cumulative inactivation in the model is comparable with that observed in the experiment. The ratio of peak current during the second pulse to

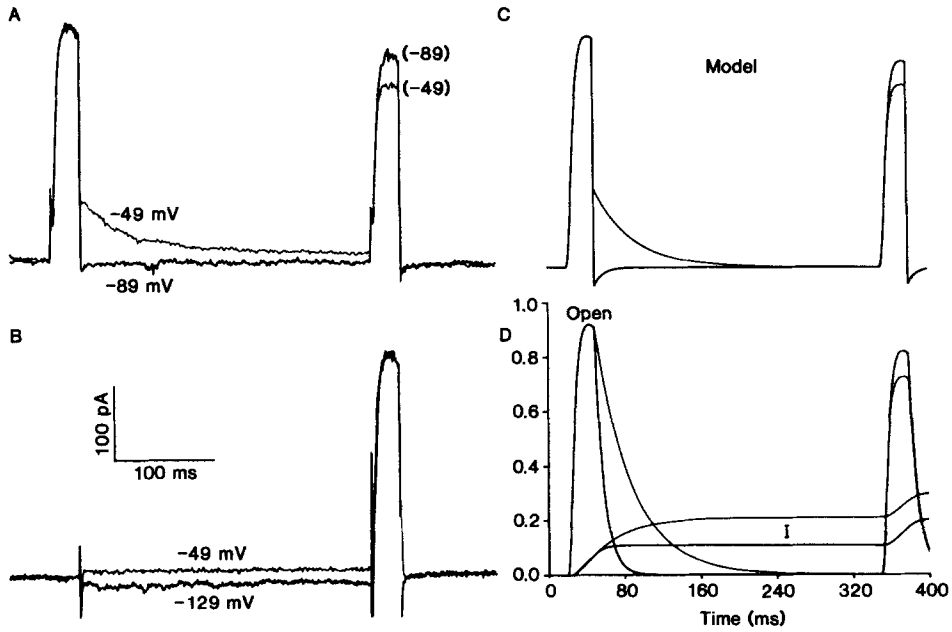

FIGURE 8. An experiment illustrating the progression of inactivation during tail currents. (*A*) A cell in 20 Ca-Ringer was held at −89 mV and two pulses to +11 mV, each 30 ms long, were applied separated by an interval of 300 ms. Two pairs of pulses are superimposed, with the potential held at −89 mV in the interpulse interval in one (*darker line*), and at −49 mV in the other (*lighter line*). The tail current is much slower at −49 mV than at −89 mV (which is just negative to the reversal potential and hence the tail is hard to see). The second test pulse to +11 mV is labeled with the potential of the interval. There was deeper cumulative inactivation when the membrane was held at −49 mV than at −89 mV between pulses, indicating that K^+ channels continue to inactivate during the tail current (see text). The cell was allowed to recover at least 1 min at −89 mV between pulses. Pipette solution KF + KCl, 20.6°C, cell no. 470. (*B*) The possibility that enhanced cumulative inactivation is due to closed channels inactivating at −49 mV is ruled out by repeating the protocol in *A* omitting the first pulse. The potential was stepped to either −49 or −129 mV (at which potential the tails are even faster than at −89 mV) for 300 ms, the same duration as the interpulse interval in *A*. The subsequent test pulse to +11 mV elicits superimposable currents, indicating that there was negligible inactivation of closed channels during this duration pulse. Not shown: no effect on the test current was detected for prepulse potentials over the range −129 to −49 mV in 20-mV increments. Calibration bars apply to both *A* and *B*. (*C*) Currents calculated with the coupled model using the same voltage pulse protocol as in *A*. As in *A*, the dark line indicates the currents when the potential during the interval was −89 mV, the lighter line −49 mV. The rate constants of inactivation were derived from τ and R measured in this cell, 250 ms and 0.02, respectively. The currents are in arbitrary units, and the timebase is identical to that in D. (*D*) Time course of probabilities of occupancy of the open state and the inactivated state for the calculated currents in *C*. The open probability rapidly rises during the simulated pulse to +11 mV, and declines after repolarization, but the closing rate at −49 mV (*lighter lines*) is smaller (i.e., slower) than at −89 mV (*darker line*). The occupancy of the inactivated state (labeled *I*) is identical during the depolarizing pulse, and continues to increase during the tail current. Since channels stay open longer at −49 mV than at −89 mV, more channels inactivate, reducing the fraction of channels available to open during the second depolarizing pulse.

that of the first pulse is 0.88 (data) and 0.89 (model) when the interpulse potential was −89 mV and 0.75 (data) and 0.79 (model) when the interpulse potential was −49 mV. The way in which inactivation is enhanced during tail currents at more positive potentials is illustrated in Fig. 8 *D*. The occupancies of the open and inactivated states during the calculated currents in Fig. 8 *C* are shown. Some channels inactivate during the first depolarizing pulse, but open channels continue to inactivate during the tail current. This progressive inactivation is much more pronounced during the tail current at −49 mV (*lighter lines*), about doubling the fraction of channels inactivated by the start of the second pulse.

An alternative explanation of the experiment in Fig. 8 might be that it reflects a rapid transition from a shallow closed state to an inactivated state. When the membrane is held at more positive potentials in the interval between the two pulses, many channels might not return to the deepest closed state (C_1 in the present model), but might occupy "shallow" closed states adjacent to or near the open state (e.g., C_3 or C_4). When the second pulse is applied, the initial conditions would then differ in that K^+ channels might be distributed among various closed states differently. The experiment in Fig. 9 *A* does not support this explanation. Here pulse trains were given in which K^+ channels were opened and then allowed to close at different rates by repolarizing to different potentials. As shown in Fig. 9, *inset*, each element of the train consisted of a brief "prepulse" to +10 mV which activates g_K followed immediately by a 200-ms "postpulse" to a potential at which most channels close. The inactivation which accumulated as a result of a given pulse structure was evaluated by the peak test K^+ current during the 20th pulse of the train. More inactivation accumulated when the postpulse potential was more positive, where channels close more slowly (−60 mV compared with −110 mV). Since the membrane was held at −90 mV between pulses in the train, each depolarizing prepulse in all trains was given from the same potential. If transitions between closed and open states reach equilibrium during the ~800 ms at −90 mV between pulses, then the dependence of accumulation of inactivation on the postpulse potential reflects enhancement of inactivation during the tail current.

Fig. 9 also addresses a different interpretation of Fig. 8: namely that the effect of interpulse potential on the subsequent test current might reflect voltage-dependence of the rate of recovery from the closed inactivated state Z_r. In this interpretation, the test current after 300 ms at −89 mV reflects nearly complete recovery from Z_r, while much less recovery occurred at −49 mV. In the experiment in Fig. 9, however, the membrane was held at −90 mV for ~800 ms after all postpulses. If recovery from Z_r were rapid at −90 mV, then the postpulse potential should have had little effect on the accumulation of inactivation, in contrast to what was actually observed.

It has been assumed that the rate of inactivation is voltage-independent in calculations using the coupled model. If this is true, then the degree to which inactivation accumulates in pulse trains like those in Fig. 9 *A* should be relatable directly to the total time that channels are open, rather than potential. This idea is tested in the graph in Fig. 9 *B*, in which the current elicited by the 20th pulse of the train is plotted as a function of the integral over time of the estimated open channel probability throughout both prepulse and postpulse ("cumulative open time," see

legend). When the postpulse potential (labeled) is more positive, the tail current is slower and more inactivation accumulates, that is, the current during the 20th pulse is smaller. When the prepulse to +10 mV is shortened from 30 (▲) to 10 ms (▼), less inactivation accumulates for a given postpulse potential. Also with shorter prepulses (▼) the extent of accumulated inactivation depends more strongly upon postpulse potential, since a greater fraction of the total inactivation takes place during the tail

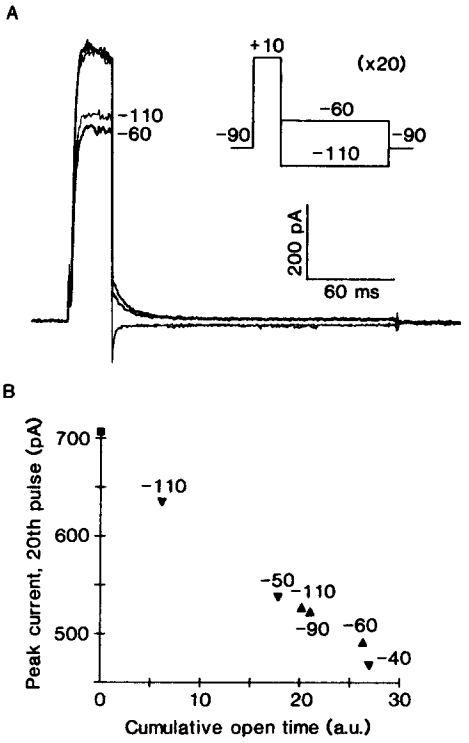

FIGURE 9. Accumulation of inactivation during pulse trains depends on the length of time channels are open, not on potential. (*A*) Pulse trains consisting of a 30-ms depolarizing prepulse to +10 mV followed by 200-ms postpulses to different potentials at which most channels close, were applied at 1 Hz. Currents elicited by the first and twentieth pulses are superimposed for trains in which the membrane was held at −60 mV (*dark lines*) or −110 mV (*lighter lines*) during the postpulse. The currents during the first prepulse in each train superimpose, but the tail current is slower at −60 mV and the degree to which inactivation accumulates is greater, as can be seen by the twentieth pulses (labeled with the postpulse potential). (*B*) The peak current during the twentieth prepulse to +10 mV is plotted against the "cumulative open time" of K^+ channels during both the brief depolarization and the tail current. "Cumulative open time" in arbitrary units was determined by integrating the current during the first pulse to +10 mV of each train, and adding the integral of the tail current (baseline subtracted) after scaling for the difference in driving force, estimated as the ratio of the current at the end of the depolarizing pulse to the instantaneous current at the start of the tail current. The depolarizing prepulse was 30 (▲) or 10 ms long (▼). The postpulse potentials are given near each data point. The square on the ordinates shows the average peak current during the first prepulse to +10 mV of each train. Ringer solution in the bath, pipette solution KCH_3SO_3, 21.7°C, cell no. 440.

current. However, when pulse protocols giving rise to similar cumulative open times are compared, the degree of inactivation is similar regardless of prepulse duration or postpulse potential. These data only indirectly reflect the rate of open channel inactivation, but to a first approximation they indicate that over a wide voltage range the likelihood of a K^+ channel inactivating depends closely upon whether the channel is open and not on membrane potential.

DISCUSSION

Inactivation Mechanisms in Other Cells

Inactivation appears to be a common feature of K^+ currents in a variety of preparations, as discussed in the Introduction. Inactivation also appears to vary widely when quantitative comparisons are made. The extent to which conclusions reached about inactivation of K^+ currents in type II cells might also apply to K^+ currents in other cells can ultimately be answered only by studying each K^+ channel type in every preparation. Nevertheless, K^+ currents in a number of preparations share at least some of the following characteristics with those in type II cells: (*a*) τ is practically voltage-independent when g_K is fully activated, (*b*) recovery is much slower than onset of inactivation, (*c*) increased $[Ca^{2+}]_o$ enhances inactivation, (*d*) increased $[K^+]_o$ diminishes inactivation, (*e*) cumulative inactivation and delayed or nonmonotonic recovery kinetics can be seen, (*f*) steady-state inactivation is significant only at potentials at which g_K is activated. The inactivation mechanism of squid delayed rectifier channels differs in being unaffected by increased $[K^+]_o$ (Clay, 1989) or $[Ca^{2+}]_o$ (Inoue, 1981), and in having rapid recovery kinetics at negative potentials (Chabala, 1984). The inactivation of A-currents differs in that τ has a bell-shaped voltage dependence with recovery roughly as rapid as onset of inactivation (Conner and Stevens, 1971*b*; Neher, 1971; Strong, 1984). Of the above characteristics of inactivation, several (specifically *a*, *b*, *d*, and *f*) also apply to the block of K^+ channels by internal quaternary ammonium ions (Armstrong, 1969, 1971; Armstrong and Hille, 1972); the model proposed by Armstrong (1969) to describe this block has been applied in this paper to K^+ channel inactivation.

There are some similarities between inactivation of sodium channels and inactivation of K^+ channels. Details of macroscopic Na^+ current kinetics have been cited as evidence for coupling of inactivation to activation (e.g., Hoyt, 1963; Goldman and Schauf, 1972; Bezanilla and Armstrong, 1977; reviewed by Goldman, 1976; Meves, 1978; but cf. Bean, 1981). It has been suggested that most of the voltage dependence of inactivation arises from coupling to activation (Armstrong and Bezanilla, 1977). Single-channel measurements indicate that inactivation of open sodium channels is relatively voltage-independent, and that the decay of macroscopic currents derives most of its voltage dependence from coupling to activation (Aldrich et al., 1983; but cf. Vandenberg and Horn, 1984), although sodium channels can inactivate without first opening (Horn et al., 1981; Horn and Vandenberg, 1984).

Other Models

Argibay (1974) considered several forms of coupled models for inactivation of K^+ currents in skeletal muscle. Two models of K^+ channel gating based upon single-channel measurements have been proposed, in which inactivated or "absorbing" states are reached from closed states only through the open state or states (Standen et al., 1985; Hoshi and Aldrich, 1988). These models are generally compatible with the present one.

Recently Clark et al. (1988) presented evidence for a rapid component of inactivation during the rising phase of K^+ currents in rabbit atrial cells. Pulse pairs were applied in which the duration of the first pulse was varied with a constant interval

between pulses. Inactivation determined from the peak of the second pulse revealed a rapid phase which was faster than the overt inactivation of open channels seen with a single depolarizing pulse. This phenomenon was shown to be compatible with the Aldrich model (1981) in which closed channels inactivate faster than do open channels. However, simulations of their experiment show that this phenomenon can also occur with the coupled model (data not shown). In the present model the rapid early phase of inactivation is due to the progression of inactivation of open channels during the interval between pulses, which for short pulses contributes substantially to the inactivation estimated by the second test pulse. As found by Clark et al. (1988), the coupled model with no $C \rightarrow I$ transitions allowed predicts an initial delay, but this lasts only until most channels open.

Implications of the Coupled Model

Inactivation of delayed recifier K^+ currents in rat alveolar type II cells in Ringer, K-Ringer, and 20 Ca-Ringer exhibits several behaviors which suggest that (*a*) inactivation and activation are coupled, (*b*) inactivation of closed channels takes place slowly, if at all, and (*c*) open channels inactivate relatively rapidly at all potentials, even at potentials negative to those at which K^+ channels open, and at which there is no detectable steady-state inactivation. These features were incorporated into a simple model with only one inactivated state. Both inactivation and recovery rate constants were made completely voltage-independent. Because K^+ currents inactivate during depolarization and recover upon hyperpolarization, the idea that inactivation is completely voltage-independent seems counterintuitive. Therefore various calculations were done with the model to see how well a model with these constraints could reproduce the main features of the data. Several general conclusions can be drawn:

(*a*) The coupled model, with voltage-independent inactivation, predicts that the observed time constant of current decay during depolarizing steps will be practically constant at positive potentials, but will be much slower at potentials where the g_K is only partially activated. If p is the steady-state probability of activation at a given potential, then τ is given by $1/(hp + j)$, making the assumption that $(\alpha + 4\beta) \gg h, j$ (Bernasconi, 1976). Thus where $p \rightarrow 1$, $\tau \approx 1/(h + j)$ and mainly reflects h, since $h > j$. But at more negative potentials as $p \rightarrow 0$, $\tau \rightarrow 1/j$ and since j is small, τ is large. This prediction compares well with the observed data in type II cells for all three external solutions studied (Fig. 2). Similarly, in many other preparations τ (in some cases, the faster component where more than one is present) is strongly voltage-dependent only at potentials at which the g_K is incompletely activated, and practically voltage-independent at potentials at which the g_K is fully activated (Schwarz and Vogel, 1971; Argibay, 1974; Aldrich et al., 1979; Inoue, 1981; Ypey and Clapham, 1984; Cahalan et al., 1985; Gallin and Sheehy, 1985; Deutsch et al., 1986; Maruyama, 1987; DeCoursey et al., 1987; Clark et al., 1988; Martynyuk and Teslenko, 1988; Grissmer and Cahalan, 1989).

(*b*) By the same reasoning, at potentials negative to those at which the g_K is activated, recovery from inactivation is predicted by the model to be quite slow. Slow recovery from inactivation, in comparison with the more rapid onset of inactivation during depolarizing pulses (where most channels open) has been recognized in

many preparations, and is one of the distinguishing characteristics of "delayed rectifier" K^+ channel inactivation (e.g., Heistracher and Hunt, 1969*b*; Argibay, 1974; Kostyuk et al., 1975; Adrian and Rakowski, 1978; Aldrich et al., 1979; Ruben and Thompson, 1984; Ypey and Clapham, 1984; Fukushima et al., 1984; Cahalan et al., 1985; Gallin and Sheehy, 1985; Maruyama, 1987). This type of behavior is implicit in the coupled model with voltage-independent rate constants governing inactivation, given that $h > j$.

(*c*) If h and j are both completely voltage-independent, then the estimate of j from τ and R measured during depolarizing pulses should allow prediction of the rate of recovery from inactivation at negative potentials. Table II shows that j was significantly greater in K-Ringer than in Ringer, so recovery at negative potentials ($\approx 1/j$) would be expected to be more rapid in K-Ringer. This requirement is qualitatively consistent with the facilitation of recovery by increased $[K^+]_o$ (Ruben and Thompson, 1984; Kostyuk and Martynyuk, 1988; Martynyuk and Teslenko, 1988); however, recovery time constants appear to be more strongly voltage-dependent than given by the model. That recovery in many preparations has a multiexponential time course indicates that more complex models will be required. Ruben and Thompson (1984) concluded that elevated $[K^+]_o$ increased the fraction of the g_K which recovered via the more rapid of two components of recovery.

(*d*) An obvious implication of the model is that K^+ channels should be inactivated in the steady-state only at potentials at which they have a finite probability of opening. The data in Figs. 4 and 5 suggest that if direct $C \rightarrow I$ transitions take place, the rate of this process is very slow compared with $O \rightarrow I$ at more positive potentials. Because the $C \rightarrow I$ transition occurs only to a small extent at potentials negative to those which open channels, it is hard to characterize. It is also possible that the slow and partial inactivation detected at subthreshold potentials in some experiments may instead reflect $C \rightarrow O \rightarrow I$ transitions which occur too infrequently to be observable as macroscopic current.

(*e*) In a strictly coupled model, inactivated channels must return to closed states through the open state. This requirement would result in a slow "tail" current upon repolarization from a pulse which inactivated most of the g_K. Such a current was not found by Argibay (1974), who concluded that an electrically silent $I \rightarrow C$ transition must be allowed. However, the amplitude of such a current would be extremely small. Using the coupled model and "typical" parameters for K-Ringer ($\tau = 450$ ms and $R = 0.28$), where the more rapid recovery rate and the larger driving force compared with Ringer create more favorable conditions for observing such a "tail" of recovery from inactivation, the amplitude of the tail ranges from 0.0015 at -120 mV to 0.012 at -40 mV, expressed as a fraction of the total g_K. The time course would essentially follow $1/j$, which is the slowest rate constant in the model. In a few type II cells in K-Ringer a small slow inward tail component was seen (e.g., Fig. 4 *B*) but in other cells no such component could be detected.

(*f*) The voltage independence of inactivation assumed in the coupled model implies that some channels will inactivate during tail currents. Since the rate of inactivation, h, is smaller in K-Ringer than in Ringer, tail currents should decay more slowly, since fewer channels will inactivate. Qualitatively compatible with this prediction, tail currents in several preparations decay more slowly as $[K^+]_o$ is increased

(Swenson and Armstrong, 1981; Cahalan et al., 1985; Matteson and Swenson, 1986). This phenomenon has been interpreted as evidence that K^+ channels cannot close when occupied by a permeant ion (Swenson and Armstrong, 1981). The extent to which inactivation would accelerate tail currents depends on the relative rates of channel closing and inactivation (4β and h in the present model). For example, in the model (assuming voltage-independent h) with τ 300 ms and R 0.06, the tail current time constant at -50 mV is 20% slower (63.3 vs. 52.8 ms) if inactivation is removed by setting h to 0, but only 3% slower (9.26 vs. 9.00 ms) at -100 mV where the closing rate is faster. Since elevated $[K^+]_o$ slows τ_{tail} by about the same proportion over a wide range of voltage within which τ_{tail} varies substantially (Cahalan et al., 1985; Matteson and Swenson, 1986), it seems likely that the mechanism of the slowing is not via an effect on inactivation.

Implications of the Coupled Model for Experimental Measurements

It is common practice to estimate the total number of K^+ channels in a preparation by dividing the maximum observable g_K by the unitary conductance. The result will always be a substantial underestimate in the Aldrich model, because a significant fraction of channels inactivate directly from the closed state during a depolarizing pulse. The coupled model predicts that observable K^+ currents will more closely reflect the total number of K^+ channels present, subject to the constraint that applies to either model: during large depolarizations the open probability may approach a limit less than unity.

The meaning of "steady-state inactivation" in the coupled model is complicated because the $C \leftrightarrow I$ equilibrium and the $O \leftrightarrow I$ equilibrium may have (and apparently do have) very different voltage-dependencies. Closed channels inactivate at most only slowly and at relatively positive potentials; open channels inactivate relatively rapidly over a wide voltage range. Radically different "steady-state" inactivation–voltage relationships will result from different experimental protocols.

Limits of the Model

The model presented clearly represents an oversimplification in several respects. For example, slow $C \rightarrow I$ transitions may take place, and have been reported in other preparations (Fukushima et al., 1984; Deutsch et al., 1986). In human T lymphocytes inactivation can be demonstrated only 5–8 mV negative to the threshold for g_K activation when 4-s prepulses are used, but up to 25 mV negative to threshold when >2-min prepulses are used (Deutsch et al., 1986). Since in type II cells any $C \rightarrow I$ transitions occur in a voltage range near that of activation, and are quite slow, this transition has been neglected in the model. In many preparations including the present one, the onset and recovery from inactivation under certain conditions are best described by at least two exponentials (references cited in Introduction). Thus, a more complete model would likely need at least two inactivated states or an additional open state. Simply adding one or more pathways between C_n and I would not generate an additional time constant of relaxation, because these would be parallel pathways (Bernasconi, 1976).

The main property of inactivation of the g_K which is not generally predicted by the simple coupled model is that the relaxation of the inactivation mechanism at

potentials negative to those at which K^+ channels open is voltage-dependent, becoming faster at more negative potentials (Heistracher and Hunt, 1969*b*; Argibay, 1974; Adrian and Rakowski, 1978; Ruben and Thompson, 1984; Chabala, 1984; Cahalan et al., 1985; Clay, 1989). In the present study, the apparent rate constants of inactivation and recovery, h and j, were both practically voltage-independent when estimated at positive potentials, and Fig. 9 does not support strong voltage dependence of h even at quite negative potentials. In the simple model, coupling of recovery with deactivation results in some acceleration of the recovery time constant at more negative potentials, but not to the extent reported. It may be possible to reconcile the relative voltage independence of the onset of inactivation with the voltage dependence of recovery by an additional inactivated state as proposed above, e.g.:

$$C_{1\text{–}4} \rightleftharpoons O \underset{j}{\overset{h}{\rightleftharpoons}} I_1 \underset{j'}{\overset{h'}{\rightleftharpoons}} I_2.$$

Another model, similar to models proposed for sodium channel inactivation (Armstrong and Bezanilla, 1977) and skeletal muscle charge movement (Brum et al., 1988), suggested to me by Eduardo Rios, which might enable a more complete description of the data is:

$$\begin{array}{ccccc} & & I_1 & \rightleftharpoons & I_2 \\ & & \Vert & & \Vert \\ C_{1\text{–}3} & \rightleftharpoons & C_4 & \rightleftharpoons & O \end{array}$$

Here transitions shown vertically are voltage-independent, while horizontal transitions, including those between the two inactivated states, I_1 and I_2, are voltage-dependent. This model preserves the voltage independence of both rate constants determining the overt inactivation of currents during depolarization, but could result in voltage-dependent recovery kinetics. The present results indicate that $C_4 \rightarrow I_1$ must be much slower than $O \rightarrow I_2$. Further experiments are needed to discriminate between these more complex models and to characterize the kinetics and voltage dependence of transitions between the inactivated states.

I thank Drs. Fred N. Quandt and Eduardo Rios for their helpful comments on the manuscript, Dr. Elizabeth R. Jacobs for support and collaboration in general, Mary Grover for able assistance in type II cell isolation, Verlin Giuffre and Phillip Zervos for building the temperature control unit, and Mark S. Shapiro for many helpful discussions.

This work was supported by grant HL37500 and Research Career Development Award K04-1928 from the National Institutes of Health.

Original version received 8 May 1989 and accepted version received 22 September 1989.

REFERENCES

Adrian, R. H., W. K. Chandler, and A. L. Hodgkin. 1966. Voltage clamp experiments in striated muscle fibers. *Journal of General Physiology.* 51:188*s*–192*s*.

Adrian, R. H., W. K. Chandler, and A. L. Hodgkin. 1970*a*. Voltage clamp experiments in striated muscle fibres. *Journal of Physiology.* 208:607–644.

Adrian, R. H., W. K. Chandler, and A. L. Hodgkin. 1970*b*. Slow changes in potassium permeability in skeletal muscle. *Journal of Physiology.* 208:645–668.

Adrian, R. H., and R. F. Rakowski. 1978. Reactivation of membrane charge movement and delayed potassium conductance in skeletal muscle fibres. *Journal of Physiology.* 278:533–557.

Aldrich, R. W. 1981. Inactivation of voltage-gated delayed potassium current in molluscan neurons: a kinetic model. *Biophysical Journal.* 36:519–532.

Aldrich, R. W., D. P. Corey, and C. F. Stevens. 1983. A reinterpretation of mammalian sodium channel gating based on single channel recording. *Nature.* 306:436–441.

Aldrich, R. W., P. A. Getting, and S. H. Thompson. 1979. Inactivation of delayed outward current in molluscan neurone somata. *Journal of Physiology.* 291:507–530.

Alving, B. O. 1969. Differences between pacemaker and nonpacemaker neurons of *Aplysia* on voltage clamping. *Journal of General Physiology.* 54:512–531.

Argibay, J. A. 1974. The potassium conductance of the skeletal muscle fibre membrane. Ph.D. thesis. University of Glasgow, Scotland.

Argibay, J. A., and O. F. Hutter. 1973. Voltage-clamp experiments on the inactivation of the delayed potassium current in skeletal muscle fibres. *Journal of Physiology.* 232:41P–43P.

Argibay, J. A., O. F. Hutter, and J. R. Slack. 1973. Consecutive activation and inactivation of the delayed rectifier in skeletal muscle fibres. *Journal of Physiology.* 237:46P–47P.

Armstrong, C. M. 1969. Inactivation of the potassium conductance and related phenomena caused by quaternary ammonium ion injection in squid axons. *Journal of General Physiology.* 54:553–575.

Armstrong, C. M. 1971. Interaction of tetraethylammonium ion derivatives with the potassium channels of giant axons. *Journal of General Physiology.* 58:413–437.

Armstrong, C. M., and F. Bezanilla. 1977. Inactivation of the sodium channel. II. Gating current experiments. *Journal of General Physiology.* 70:567–590.

Armstrong, C. M., and B. Hille. 1972. The inner quaternary ammonium ion receptor in potassium channels of the node of Ranvier. *Journal of General Physiology.* 59:388–400.

Beam, K. G., and P. L. Donaldson. 1983. A quantitative study of potassium channel kinetics in rat skeletal muscle from 1 to 37°C. *Journal of General Physiology.* 81:485–512.

Bean, B. P. 1981. Sodium channel inactivation in the crayfish giant axon: must channels open before inactivating? *Biophysical Journal.* 35:595–614.

Bernasconi, C. F. 1976. Relaxation Kinetics. Academic Press, Inc., New York. 288 pp.

Bennett, M. V. L., and H. Grundfest. 1966. Analysis of depolarizing and hyperpolarizing inactivation responses in gymnotid electroplaques. *Journal of General Physiology.* 50:141–169.

Bezanilla, F., and C. M. Armstrong. 1977. Inactivation of the sodium channel. I. Sodium current experiments. *Journal of General Physiology.* 70:549–566.

Brum, G., R. Fitts, G. Pizarro, and E. Rios. 1988. Voltage sensors of the frog skeletal muscle membrane require calcium to function in excitation-contraction coupling. *Journal of Physiology.* 398:475–505.

Cahalan, M. D., K. G. Chandy, T. E. DeCoursey, and S. Gupta. 1985. A voltage-gated potassium channel in human T lymphocytes. *Journal of Physiology.* 358:197–237.

Chabala, L. D. 1984. The kinetics of recovery and development of potassium channel inactivation in perfused squid (*Loligo pealei*) giant axons. *Journal of Physiology.* 356:193–220.

Clark, R. B., W. R. Giles, and Y. Imaizumi. 1988. Properties of the transient outward current in rabbit atrial cells. *Journal of Physiology.* 405:147–168.

Clay, J. R. 1989. Slow inactivation and reactivation of the K^+ channel in squid axons: a tail current analysis. *Biophysical Journal.* 55:407–414.

Cole, K. S., and J. W. Moore. 1960. Potassium ion current in the squid giant axon: dynamic characteristic. *Biophysical Journal.* 1:1–14.

Conner, J. A., and C. F. Stevens. 1971*a*. Inward and delayed outward membrane currents in isolated neural somata under voltage clamp. *Journal of Physiology.* 213:1–19.

Conner, J. A., and C. F. Stevens. 1971*b*. Voltage clamp studies of a transient outward membrane current in gastropod neural somata. *Journal of Physiology.* 213:21–30.

Cota, G., and C. M. Armstrong. 1988. Potassium channel "inactivation" induced by soft-glass patch pipettes. *Biophysical Journal.* 53:107–109.

DeCoursey, T. E., K. G. Chandy, S. Gupta, and M. D. Cahalan. 1984. Voltage-gated K^+ channels in human T lymphocytes: a role in mitogenesis? *Nature.* 307:465–468.

DeCoursey, T. E., K. G. Chandy, S. Gupta, and M. D. Cahalan. 1985. Voltage-dependent ion channels in T-lymphocytes. *Journal of Neuroimmunology.* 10:71–95.

DeCoursey, T. E., K. G. Chandy, S. Gupta, and M. D. Cahalan. 1987. Two types of potassium channels in murine T lymphocytes. *Journal of General Physiology.* 89:379–404.

DeCoursey, T. E., E. R. Jacobs, and M. R. Silver. 1988. Potassium channels in rat type II alveolar epithelial cells. *Journal of Physiology.* 395:487–505.

Deutsch, C., D. Krause, and S. C. Lee. 1986. Voltage-gated potassium conductance in human T lymphocytes stimulated with phorbol ester. *Journal of Physiology.* 372:405–423.

Dubois, J. M. 1981. Evidence for the existence of three types of potassium channels in the frog Ranvier node membrane. *Journal of Physiology.* 318:297–316.

Duval, A., and C. Leoty. 1978. Ionic currents in mammalian fast skeletal muscle. *Journal of Physiology.* 278:403–423.

Eckert, R., and H. D. Lux. 1977. Calcium-dependent depression of a late outward current in snail neurons. *Science.* 197:472–475.

Ehrenstein, G., and D. L. Gilbert. 1966. Slow changes of the potassium permeability in the squid giant axon. *Biophysical Journal.* 6:553–566.

Fernandez, J. M., A. P. Fox, and S. Krasne. 1984. Membrane patches and whole-cell membranes: a comparison of electrical properties in rat clonal pituitary (GH_3) cells. *Journal of Physiology.* 356:565–585.

Frankenhaeuser, B. 1963. A quantitative description of potassium currents in myelinated nerve fibres of *Xenopus laevis*. *Journal of Physiology.* 169:424–430.

Frankenhaeuser, B., and A. L. Hodgkin. 1957. The action of calcium on the electrical properties of squid axons. *Journal of Physiology.* 137:218–244.

Frankenhaeuser, B., and B. Waltman. 1959. Membrane resistance and conduction velocity of large myelinated nerve fibres from *Xenopus laevis*. *Journal of Physiology.* 148:677–682.

Fukushima, Y., S. Hagiwara, and M. Henkart. 1984. Potassium current in clonal cytotoxic T lymphocytes from the mouse. *Journal of Physiology.* 351:645–656.

Gallin, E. K., and P. A. Sheehy. 1985. Differential expression of inward and outward potassium currents in the macrophage-like cell line J774. *Journal of Physiology.* 369:475–499.

Giles, W. R., and Y. Imaizumi. 1988. Comparison of potassium currents in rabbit atrial and ventricular cells. *Journal of Physiology.* 405:123–145.

Gilly, W. F., and C. M. Armstrong. 1982. Divalent cations and the activation kinetics of potassium channels in squid giant axons. *Journal of General Physiology.* 79:965–996.

Goldman, L. 1976. Kinetics of channel gating in excitable membranes. *Quarterly Review of Biophysics.* 9:491–526.

Goldman, L., and C. L. Schauf. 1972. Inactivation of the sodium current in *Myxicola* giant axons: evidence for coupling to the activation process. *Journal of General Physiology.* 59:659–675.

Grissmer, S., and M. D. Cahalan. 1989. Divalent ion trapping inside potassium channels of human T lymphocytes. *Journal of General Physiology.* 93:609–630.

Hagiwara, S., K. Kusano, and N. Saito. 1961. Membrane changes of *Onchidium* nerve cell in potassium-rich media. *Journal of Physiology.* 155:470–489.

Hall, A. E., O. F. Hutter, and D. Noble. 1963. Current-voltage relations of Purkinje fibres in sodium-deficient solutions. *Journal of Physiology.* 166:225–240.

Heistracher, P., and C. C. Hunt. 1969*a*. The relation of membrane changes to contraction in twitch muscle fibres. *Journal of Physiology.* 201:589–611.

Heistracher, P., and C. C. Hunt. 1969*b*. Contractile repriming in snake twitch muscle fibres. *Journal of Physiology.* 201:613–626.

Heyer, C. B., and H. D. Lux. 1976. Control of the delayed outward potassium currents in bursting pace-maker neurones of the snail, *Helix pomatia*. *Journal of Physiology.* 262:349–382.

Hodgkin, A. L., and A. F. Huxley. 1952. A quantitative description of membrane current and its application to conduction and excitation in nerve. *Journal of Physiology.* 117:500–544.

Horn, R., J. Patlak, and C. F. Stevens. 1981. Sodium channels need not open before they inactivate. *Nature.* 291:426–427.

Horn, R., and C. A. Vandenberg. 1984. Statistical properties of single sodium channels. *Journal of General Physiology.* 84:505–534.

Horrigan, F. T., M. Lucero, H.-T. Leung, T. Brismer, and W. F. Gilly. 1987. Unusual inactivation of potassium current (I_K) in cell bodies of the giant axons in "gulf" squid. *Biophysical Journal.* 51:365*a*. (Abstr.)

Hoshi, T., and R. W. Aldrich. 1988. Gating kinetics of four classes of voltage-dependent K^+ channels in pheochromocytoma cells. *Journal of General Physiology.* 91:107–131.

Hoyt, R. C. 1963. The squid giant axon: mathematical models. *Biophysical Journal* 3:399–431.

Inoue, I. 1981. Activation-inactivation of potassium channels and development of the potassium-channel spike in internally perfused squid giant axons. *Journal of General Physiology.* 78:43–61.

Kostyuk, P. G., O. A. Krishtal, and P. A. Doroshenko. 1975. Outward currents in isolated snail neurones-I. inactivation kinetics. *Comparative Biochemistry and Physiology.* 51C:259–263.

Kostyuk, P. G., and A. E. Martynyuk. 1988. Potassium outward current dependent on extracellular calcium in snail neuronal membrane. *Neuroscience.* 24:1081–1087.

Landolt-Börnstein. 1960. Zahlenwerte und Funktionen. II Band: Eigenschaften der Materie in ihren Aggregatzuständen. 7 Teil: Elektrische Eigenschaften II. K.-H. Hellwege, A. M. Hellwege, K. Schäfer, and E. Lax, editors. Springer-Verlag, Berlin. 264–266.

Lucero, M. T., and P. A. Pappone. 1989. Voltage-gated potassium channels in brown fat cells. *Journal of General Physiology.* 93:451–472.

Lüttgau, H. C. 1960. Das Kalium-Transportsystem am Ranvier-Knoten isolierter markhaltiger Nervenfasern. *Pflügers Archiv für die gesamte Physiologie des Menschen und Tiere.* 271:613–633.

Lüttgau, H. C. 1961. Weitere Untersuchungen über den passiven Ionentransport durch die erregbare Membran des Ranvierknotens. *Pflügers Archiv für die gesamte Physiologie des Menschen und Tiere.* 273:302–310.

Magura, I. S., O. A. Krishtal, and A. G. Valeyev. 1971. Behavior of delayed current under long-duration voltage clamp in snail neurons. *Comparative Biochemistry and Physiology.* 40A:715–722.

Marty, A. and E. Neher. 1983. Tight-seal whole-cell recording. *In* Single-Channel Recording. B. Sakmann and E. Neher, editors. Plenum Press, New York. 107–122.

Martynyuk, A. E., and V. I. Teslenko. 1988. Inactivation of outward potassium current dependent on extracellular Ca^+ (sic). *Neurophysiology.* (English translation of *Neurofiziologiya*). 20:436–442.

Maruyama, Y. 1987. A patch-clamp study of mammalian platelets and their voltage-gated potassium current. *Journal of Physiology.* 391:467–485.

Matteson, D. R., and R. P. Swenson. 1986. External monovalent cations that impede the closing of K channels. *Journal of General Physiology.* 87:795–816.

Meves, H. 1978. Inactivation of the sodium permeability in squid giant axons. *Progress in Biophysics and Molecular Biology.* 33:207–230.

Moore, J. W. 1959. Excitation of the squid axon membrane in isosmotic potassium chloride. *Nature.* 183:265–266.

Mounier, Y. 1979. Inactivation of the slow potassium outward current in crab muscle fibre. *Archives Internationales de Physiologie et de Biochimie.* 87:501–508.

Nakajima, S., S. Iwasaki, and K. Obata. 1962. Delayed rectification and anomalous rectification in frog's skeletal muscle membrane. *Journal of General Physiology.* 46:97–115.

Nakajima, S., and K. Kusano. 1966. Behavior of delayed current under voltage clamp in the supramedullary neurons of puffer. *Journal of General Physiology.* 49:613–628.

Neher, E. 1971. Two fast transient current components during voltage clamp on snail neurons. *Journal of General Physiology.* 58:36–53.

Neher, E., and H. D. Lux. 1971. Properties of somatic membrane patches of snail neurons under voltage clamp. *Pflügers Archiv.* 322:35–38.

Plant, T. D. 1986. The effects of rubidium ions on components of the potassium conductance in the frog node of Ranvier. *Journal of Physiology.* 375:81–105.

Quandt, F. N. 1988. Three kinetically distinct potassium channels in mouse neuroblastoma cells. *Journal of Physiology.* 395:401–418.

Robinson, R. A., and R. H. Stokes. 1965. Electrolyte Solutions. Butterworths, London. 571 pp.

Ruben, P., and S. Thompson. 1984. Rapid recovery from K current inactivation on membrane hyperpolarization in molluscan neurons. *Journal of General Physiology.* 84:861–875.

Schwarz, J. R., and W. Vogel. 1971. Potassium inactivation in single myelinated nerve fibres of *Xenopus laevis. Pflügers Archiv.* 330:61–73.

Simon, R. H., J. P. McCoy, A. E. Chu, P. D. Dehart, and I. J. Goldstein. 1986. Binding of *Griffonia simplicifolia* I lectin to rat pulmonary alveolar macrophages and its use in purifying type II alveolar epithelial cells. *Biochimica et Biophysica Acta.* 885:34–42.

Standen, N. B., P. R. Stanfield, and T. A. Ward. 1985. Properties of single potassium channels in vesicles formed from the sarcolemma of frog skeletal muscle. *Journal of Physiology.* 364:339–358.

Stanfield, P. R. 1970. The effect of the tetraethylammonium ion on the delayed currents of frog skeletal muscle. *Journal of Physiology.* 209:209–229.

Strong, J. A. 1984. Modulation of potassium current kinetics in bag cell neurons of Aplysia by an activator of adenylate cyclase. *Journal of Neuroscience.* 11:2772–2783.

Swenson, R. P., and C. M. Armstrong. 1981. K^+ channels close more slowly in the presence of external K^+ and Rb^+. *Nature.* 291:427–429.

Vandenberg, C. A., and R. Horn. 1984. Inactivation viewed through single sodium channels. *Journal of General Physiology.* 84:535–564.

Vanýsek, P. 1987. Equivalent ionic conductivities extrapolated to infinite dilution in aqueous solutions at 25°C. *In* CRC Handbook of Chemistry and Physics. R. C. Weast, editor. CRC Press, Boca Raton, FL. D-167–D-169.

White, M. M., and F. Bezanilla. 1985. Activation of squid axon K^+ channels: ionic and gating current studies. *Journal of General Physiology.* 85:539–554.

Ypey, D. L., and D. E. Clapham. 1984. Development of a delayed outward-rectifying K^+ conductance in cultured mouse peritoneal macrophages. *Proceedings of the National Academy of Sciences.* 81:3083–3087.